MODELING THE DYNAMIC BEHAVIOUR OF AXI-SYMMETRICAL FRUITS USING THE DISCRETE ELEMENT METHOD

by
H. Abbaspour-fard and J.F. Favier

Biological Systems Engineering Group
University of Newcastle
Newcastle upon Tyne, UK

Summary:

A new Discrete Element (DE) method has been developed to model the dynamic behaviour of an assembly of axi-symmetrically shaped fruits. In the new method, which we term the "multi-element" method, model fruits (taken here to also include vegetables, grains and nuts) are comprised of overlapping spheres whose centres are fixed in position relative to each other along the major axis of symmetry of the fruit. Element spheres are inscribed in the real fruit shape such that the diameter of the spheres varies with the fruit surface contour. Contact detection between two neighbouring model fruits is achieved using standard DE methods for two single spheres. The method thus takes advantage of the speed and accuracy of contact detection associated with standard DE schemes employing single spheres. The scheme is well suited to numerical modelling of post-harvest operations such as hopper filling and emptying, conveying, sorting and object manipulation where the produce are discrete entities with relatively round smooth surfaces.

Keywords:

Discrete Element Method, DEM, multi-element particles, dynamic behaviour, fruits, simulation

Introduction

The discrete element method (DEM) is a numerical scheme for modelling the dynamic behavior of a particulate assembly at the particle length scale. Each particle is considered as a discrete, homogeneous rigid body and Newtonian mechanics are used to determine the translational and rotational motion of each particle in the assembly over a discrete time step. Inter-particle forces are calculated based on the relative velocity of contacting particles (or particle-wall) and assumption of a small "virtual" overlapping contact. Particle velocity and position at the end of a time step are obtained through numerical integration of the computed accelerations. The method is explicit since, using the principle of causality, disturbances cannot propagate from any particle further than its immediate neighbours. Resultant forces on any particle at any time increment are determined solely by interactions with contacting neighbours. Change in the configuration of an assembly is therefore a function of the physical properties of the particles (stiffness, damping, surface properties) and the microstructure or fabric of the assembly. There is no theoretical limit on the number of particles in an assembly and simulations of the bulk behavior of real particulate systems are usually constrained by available computing speed. Simulations of assemblies containing up to 65000 2-D and 10000 3-D circular elements have been reported (Hryciw et al, 1997, Thornton and Kafui, 1997). A substantial proportion of the computation time is taken up in detection of contacts between particles. The method of contact detection employed is largely dependent on the particle shape. The fastest scheme is that associated with spheres where contact is determined directly from the distance between particle centres.

Although contact detection and computation time are very important, the critical objective in DE modeling is accurate simulation of the behavior of an assembly of real particles. The influence of particle shape on the predicted behavior is less well documented than the relationship between shape and the efficiency of contact detection. The most common element shapes used in DE models are circular discs (e.g. Cundall and Strack, 1983) or spheres (e.g. Ning et al, 1997). While spherical elements have the great advantage of computational simplicity, they also possess an inherent tendency to rotate; a feature which has been thought to be one of major sources of deviation in the simulation of non-spherical granular material (Lin and Ng, 1995). The less spherical the real particles, the greater the degree of interlocking which limits their ability to rotate. In addition, normal contact forces do not contribute to the moment acting on a spherical element as each normal contact force always acts through the centre of the element. This has the effect of weighting the rotational effect of the contact force vector towards the tangential component. These two inherent attributes of circular or spherical particles will contribute to a degradation in the accuracy of simulations of the behavior of particles which deviate to any significant degree from purely spherical.

DE models using non-spherical particle shapes have been developed including ellipses (Ting et al. 1993), ellipsoids (Lin and Ng, 1997), superquadric functions (Hogue, 1998), polygons and polyhedra (Hart et al, 1988). All of these shape representations are significantly more computationally expensive than circular or spherical shapes and, with the exception of polygons, have had limited application in DE modeling. We present here a new, computationally efficient method of modeling non-spherical, axi-symmetrical particles using overlapping spheres. The approach, which we term the "multi-element" method, employs the same constitutive laws and principles for contact detection as usually employed for systems of single spheres.

Multi-element particle model

Model particles are constructed of spheres whose centres are located on the particle axis of symmetry. Spheres may overlap and may vary in diameter along the length of the axis of symmetry. The surface of a particle is approximated by inscribing spheres such that the surface of each sphere is tangent to the surface of the particle at the point of contact. The position of each element sphere is fixed relative to the other elements within a particle. The following is a summary of the main constitutive equations of the model. Derivation of the equations is given in Favier et al (1999).

Consider two particles, each comprised of two spherical elements of the same diameter, in contact at point c as shown in Fig 1 (only two dimensions are shown but the theory is developed for three dimensions). The global position of each particle is determined at its centroid by its global position vector $\mathbf{r_{p(G)}}$. The relative position vector between the particle centroid and the centre of an element sphere $\mathbf{d_{ps}}$ is known *a priori* because the position of each sphere within a particle is determined in advance. The position of contact point, c, on each element sphere relative to the particle centroid is

$$\mathbf{l_{pc}} = \mathbf{d_{ps}} + \mathbf{r_{psc}} \tag{1}$$

where $\mathbf{r_{psc}}$ is calculated from the global co-ordinate of the centre of the contacting spheres and subscripts p and s refer to particle and sphere respectively. Contact detection between two multi-element particles is based on detection of contacts between their element spheres. Contact is detected if the distance between the centres of the two contacting element spheres is equal to or less than the sum of their radii. Any suitable method may be used to optimise the search for contacts as are standard in DE codes employing single spheres except that in this case contacts are determined particle by particle rather than independently for each sphere.
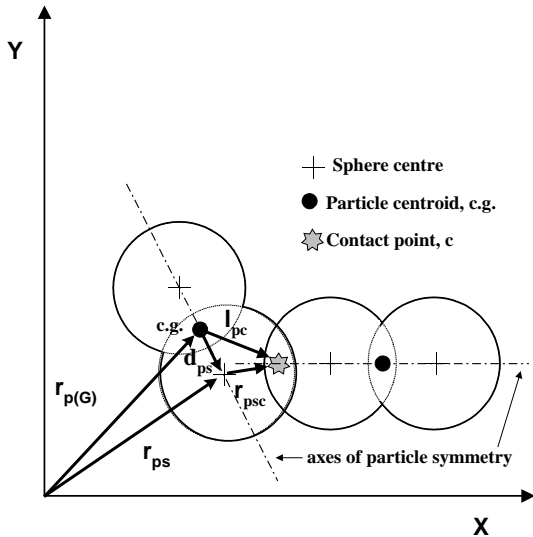
Fig 1. Schematic of contact between two multi-element axi-symmetrical particles, each comprising two element spheres of the same diameter

The total moment acting on the particle is comprised of the moments due normal and tangential forces acting on the element spheres. Through a process of transferral of moments acting on the spheres to the centroid of the particle the total moment acting on the particle is

$$\mathbf{M_p} = \sum_{s=1}^{S}\left[\left(\mathbf{d_{ps}}\times\mathbf{f_{ps}}\right)+\sum_{c=1}^{C}\left(\mathbf{r_{psc}}\times\mathbf{f_{t_{psc}}}\right)\right] \tag{2}$$

where $\mathbf{f_{ps}}$ is the sum of the contact forces acting on an element sphere transferred to the centre of the sphere, $\mathbf{f_{tpsc}}$ is the tangential component of a contact force, S is the total number of element spheres within the particle and C is the total number of contacts on an element sphere.

The total out-of-balance force acting on the particle is the vectorial sum of contact forces acting on its element spheres

$$\mathbf{f_p} = \sum_{s=1}^{S} \sum_{c=1}^{C} \mathbf{f_{psc}} \tag{3}$$

Once the total force and moment acting on a particle have been determined, Newton's second law of motion is used to calculate the translational and rotational accelerations of a particle. Using a central difference scheme and explicit numerical integration, and assuming accelerations and velocities during a certain time-step remain constant, the translational and rotational velocity of the particle are then computed

$$\mathbf{v_p}^{\left(N+\frac{1}{2}\right)} = \mathbf{v_p}^{\left(N-\frac{1}{2}\right)} + \left(\frac{\mathbf{f_p}^N}{m_p} + \mathbf{g}\right)\Delta t \tag{4}$$

$$\mathbf{w_p}^{\left(N+\frac{1}{2}\right)} = \mathbf{w_p}^{\left(N-\frac{1}{2}\right)} + \alpha_{\mathbf{p}(G)}^N \Delta t \tag{5}$$

where m_p is the particle mass. Due to the non-sphericity of the particles it is necessary to consider the mass moment of inertia when calculating the rotational acceleration of a particle. This requires transformation of the local rotational acceleration to the global reference frame which is achieved by rotation of the inertia tensor of the particle as discussed in Favier et al (1999). Using (5) and integrating over the time-step the new position of the particle is

$$\mathbf{r}_{\mathbf{p}(G)}^{(N+1)} = \mathbf{r}_{\mathbf{p}(G)}^N + \mathbf{v_p}^{\left(N+\frac{1}{2}\right)}\Delta t \tag{6}$$

Finally the position and rotational velocity of the element spheres are determined by calculation of the direction cosines. The absolute velocity of the centre of an element sphere with respect to the global axes is

$$\mathbf{v_{ps}} = \mathbf{v_p} + \left(\mathbf{w_p} \times \mathbf{d_{ps}}\right) \tag{7}$$

The magnitude of $\mathbf{d_{ps}}$ which locates the centre of sphere s with respect to the particle centroid, is fixed but its direction will be changed due to particle rotation. The vector can be written in terms of its unit vector $\mathbf{n}$ as

$$\mathbf{d_{ps}} = \left|\mathbf{d_{ps}}\right|\mathbf{n} \tag{8}$$

An approximation is required due to the discrete form of differentiation of the unit position vector. In order for this vector to remain of unit length after a rotation it is normalised by its magnitude. The global position vector of sphere s is then

$$\mathbf{r}_{\mathbf{ps}_{new}} = \mathbf{r}_{\mathbf{p}(G)} + \mathbf{d}_{\mathbf{ps}_{new}} \tag{9}$$

where $\mathbf{d_{ps(new)}}$ is the normalised local position vector. The algorithm applies to each element sphere in a particle which may contain any number of spheres. Completion of the update of the position and velocity of each element sphere completes the calculation cycle for a particle over a single time-step.

Experimental validation of the model

The model was validated numerically and experimentally. The numerical validation involved comparison between analytical and model calculations of contact forces with multi-element particles at rest and sliding along an inclined surface. Since DEM algorithms for spheres are well established, this type of numerical validation is designed to expose systematic errors in the programme. The results showed that the code was able to closely emulate the analytical results, e.g. weight of particle at rest. While numerical validation provided evidence that the model was properly formulated it could not demonstrate that the physical model employed was adequate to predict the dynamic behavior of a non-spherical "multi-element" particle.

Materials and Methods

Experiments were conducted on 1:1 scale between experiment and simulation using approximately identically shaped particles in each. Experiments consisted of vertical displacement of an assembly of two-element particles through a narrowing orifice so that particles translated and rotated. The experimental rig comprised a flat V-shaped hopper with walls made of perspex delivering in to a flat column in which moved a motorised piston as shown in Fig 2. The walls were spaced just greater than the diameter of an element sphere which constrained particle movement to two-dimensions. Preliminary tests showed that particle rotation about their major axis was minimal during an experiment. Ten particles each comprised of two 45 mm diameter spheres overlapped by 25% of their diameter were used in each experiment. The spheres were pool balls made from phenolic resin machined flat at the point of overlap and glued together. The physical properties of the spheres are given in Table 1. The particle-particle static coefficient of friction was determined by determining the angle at which a block of three particles began to slide over another identical block. The particle-wall coefficient of friction was determined by sliding a block of particles over a sheet of perspex. The coefficient of restitution was determined by dropping a sphere from on to a rigidly fixed hemi-sphere and measuring the rebound height. The coefficient of restitution was then calculated from

$$e = (h/H)^{1/2} \qquad\qquad ….(10)$$

where H is the drop height and h is the rebound height. The value shown for e in Table 1 is the mean of 30 replicates.

Table 1: Physical properties of experimental particles

Mass	142 g
Element sphere diameter	45 mm
Static coefficient of friction (particle-particle)	0.357
Static coefficient of friction (particle-wall)	0.351
Coefficient of restitution	0.85
Poisson's ratio	0.35
Elastic modulus	6.89 GPa

In each experiment the particles were placed in the same position and orientation as that of numerical model. The particle assembly was moved at a controlled rate by moving the supporting piston downwards. The velocity of the piston was 4.6 cm/s in all experiments. The piston, drive and drive motor were mounted on a separate frame to that of the hopper to reduce transfer of vibration from the motor

to the hopper. A typical arrangement of particles at the start of an experiment is shown in Fig 2a.. The movement of particles was recorded with a camcorder at a frequency of 50 frames/s. Each frame was extracted from the video file and analysed to determine the particle co-ordinates and orientation. Each experiment was repeated five times. Two sets of experiments were carried out. In the first experiment particles were placed in the same position at the start of each run. The objective was to determine how closely the movement of each particle could be replicated, i.e. how sensitive to initial position was the subsequent behavior. In the second set of experiments the arrangement of the particles (assembly microstructure) was preserved but different particles were placed in each position in an experiment.

A numerical simulation was carried out using the measured physical properties using an identical hopper and piston geometry. The velocity of the piston used in the simulation was the same as that in the experiments. Simulations were repeated with the same initial assembly microstructure but using different values for inter-particle friction coefficient to test the influence of this parameter.

Results and discussion

The tracks of the particle centroids in the two experiments with identical initial assembly structure and particle positions are shown in Fig 3. The tracks for each particle were very similar which shows that the method of assembly construction resulted in close replication of assembly behavior. This result also suggested that in order to introduce a variation in the behavior of the assembly the positions of the particles should be alternated within the same assembly structure. This was because the experimental particles all differed in size and shape by a small amount (due to differences in the amount of overlap and positioning of element spheres) while the simulated particles were all identical. Differences in the size and shape of the real particles were not easily measurable but were implicit in the method of manufacture.

Simulations with particle friction coefficients (μ) of 0.0, 0.1, 0.2, and 0.35 (equal to the static coefficient of friction between particles) resulted in the trajectories shown in Fig 4. It can be seen that while the behavior of some particles was replicated the movement of others (e.g. particle 9) was quite different. Comparison with Fig 3 shows that the trajectories for a high coefficient of friction (μ = 0.35) and frictionless condition (μ = 0.0) are in poor agreement with the experiment. The closest match was for trajectories using a value of μ of 0.1. This is in accord with the commonly observed difference between dynamic and static friction coefficient. The magnitude of the difference between the measured value and the value giving the closest match between experiment and simulation is not relevant here (given the very small numbers of replicates and the ignoring of the potential influence of other parameters) but it does suggest that dynamic rather than static friction coefficients should be used in DE models of particle flow.

Examples of the change in the orientation of particles is shown in Fig. 5. The plots show the most divergent curves and the simulated curve for a poor match (particle 1), a reasonable match (particle 9) and a good match (particle 10) between the experimental and simulated curves. The simulated curves were all based on a value of friction coefficient of 0.1. The translation of these particles is shown in Fig. 6 which includes all experimental replicates. Again the worst match is for particle 1 and the best for particle 9. The quality of the match between the experimental and simulated tracks for the remaining particles was between these two extremes.

Consideration of both the particle translation and change in particle orientation shows that on the whole the match between experiment and simulation was very good given the noise introduced by physical replication of the particle assembly, the variation in physical particle geometry, the relatively long distance over which each

could evolve and the limited exploration of the sensitivity to the magnitude of model parameters. It can therefore be concluded that, at least on a coarse scale, the physical principles and numerical approximations in the DE model are validated by the experimental results. Although the particle shape tested represented the most simple possible multi-element shape the principle should apply for more complex shapes.

Simulations

Examples of shapes which can be represented using the axi-symmetrical multi-element method are shown in Fig 7. It can be seen that a wide range of shape representation is possible including ellipsoid, cylindrical, and irregular axi-symmetric. The degree of surface fitting depends on the number of element spheres used to create a particle. Increasing the number of element spheres per particle will reduce proportionally the overall number of particles which can handled within a particular simulation using a given level of computing power. The choice of number of element spheres will therefore depend on the application and the desired approximation to actual particle shape. The degree of approximation to the particle surface will govern the magnitude of the error in calculation of the contact force vectors. These errors have been estimated to be below 5% for many particle shapes when the average specific sphere density (i.e. the average number of spheres occupying a length equal to the mean sphere diameter) is greater than five.

Examples of the consolidation and flow of multi-element objects are shown in Fig 8. They show the potential offered by the multi-element method for discrete element modeling of assemblies of smooth surfaced objects with much greater irregularity in shape than was previously possible.

Conclusions

A new method of modeling the dynamic behavior of axi-symmetrical fruits has been summarised. The method is termed the multi-element approach and uses overlapping spheres to represent fruit surface contour. The use of spheres to represent a particle takes advantage of the computational speed and accuracy of contact detection for spheres which should make the method comparable or superior in computational efficiency to alternative schemes for representing non-spherical objects. The method offers a powerful alternative to the use of instrumented spheres for determination of impact forces on fruits in handling systems. It can be used to study the mechanical behavior of fruits and vegetables during post-harvest operations with the objective of improving the design and performance of handling machinery. The model predicts normal and tangential contact forces on fruits within bulks during handling and can therefore be used to increase understanding of conditions leading to bruising and abrasion of produce.

References

Cundall, P.A. (1988), "Formulation of a three-dimensional distinct element model - Part I. A scheme to detect and represent contacts in a system composed of many polyhedral blocks", *Int. J. Rock Mechanics*, **25(3)**: 107-116.

Favier, J.F., Abbaspour-fard, M.H.; Kremmer, M. and Raji, A.O. (1999) Shape representation of axi-symmetrical, non-spherical particles in discrete element simulation using multi-element particles. *Engineering Computations*, **16(4)**: 467-480.

Hart, R., Cundall, P.A. and Lemos, J. (1988), "Formulation of a three-dimensional distinct element model – Part II. Mechanical calculations for motion and interaction of a system composed of many polyhedral blocks", *Int. J. Rock Mechanics*, **25(3):** 117-125.

Hogue, C. (1998), " Shape representation and contact detection for discrete element simulations of arbitrary geometries.", *Engineering Computations*, **15(3):** 374-390*.*

Hryciw, R.D.; Raschke, S.; Ghalib, A.M., Horner, D.A. and J.F. Peters (1997) Video tracking for experimentation of discrete element simulations of large discontinuous deformations. *Computers and Geotechnics*, **2(3):**235-253.

Lin, X. and Ng, T.T. (1995), "Short communication, contact detection algorithms for three dimensional ellipsoid in discrete element modeling.", *International Journal for Numerical Methods in Geomechanics.*, **19** : 653-659.

Lin_X and Ng, T.T. (1997), "A three-dimensional discrete element model using arrays of ellipsoids", *Geotechnique*, **47(2)**: 319-329.

Ning, Z; Boerefijn, R. and Ghadiri, M. (1997), "Distinct element simulation of impact breakage of lactose agglomerates." *Advanced Powder Technology,* **8(1):** 15-37.

Ting, J.M., Meachum, L. and Rowell, J.D. (1995), "Effect of particle shape on the strength and deformation mechanisms of ellipse-shaped granular assemblages"*, Engineering Computations,* **12:** 99-108.

Thornton, C. and Kafui, K.D. (1997), " Numerical simulations of granular flow in hoppers and silos.", *2ⁿᵈ Israel Conference for Conveying and Handling of Particulate Solids.,* Jerusalem, Israel, May 26-28.
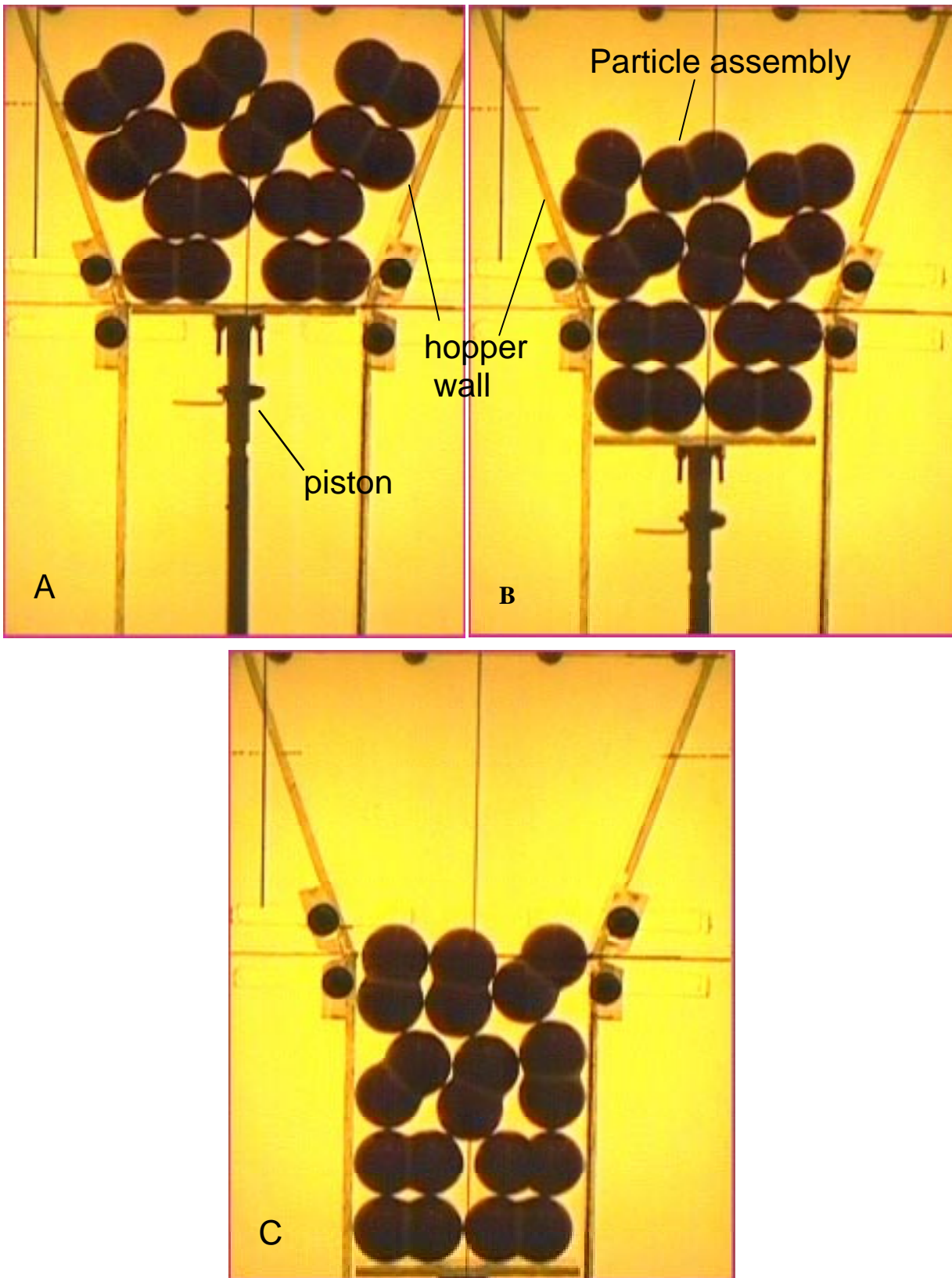
Fig 2 Section of experimental apparatus showing three images from (a) the start, (b) during, and (c) the end of an experimental run.
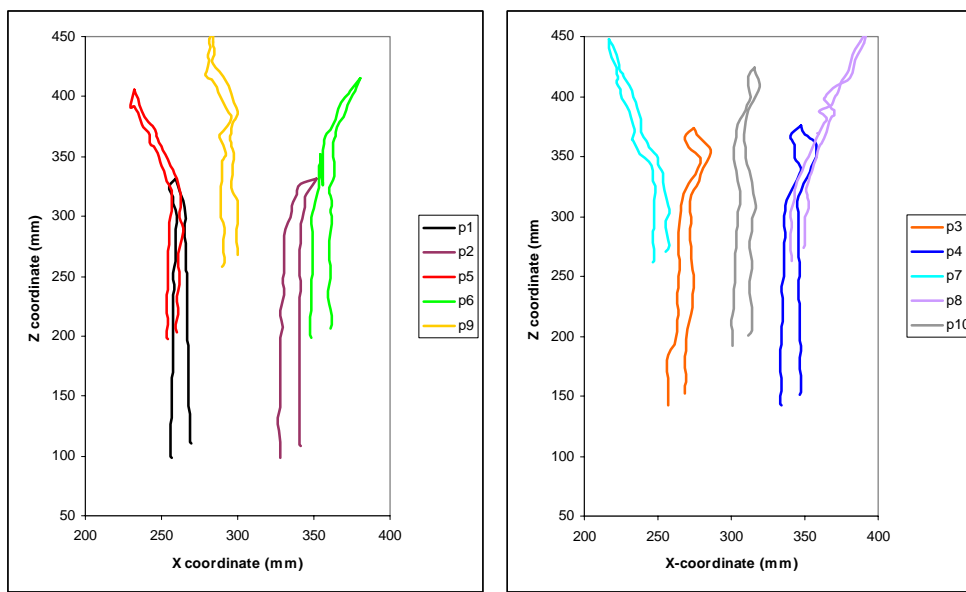
Fig. 3 Tracks of the centroids of particles in two experiments using an identical arrangement of particles
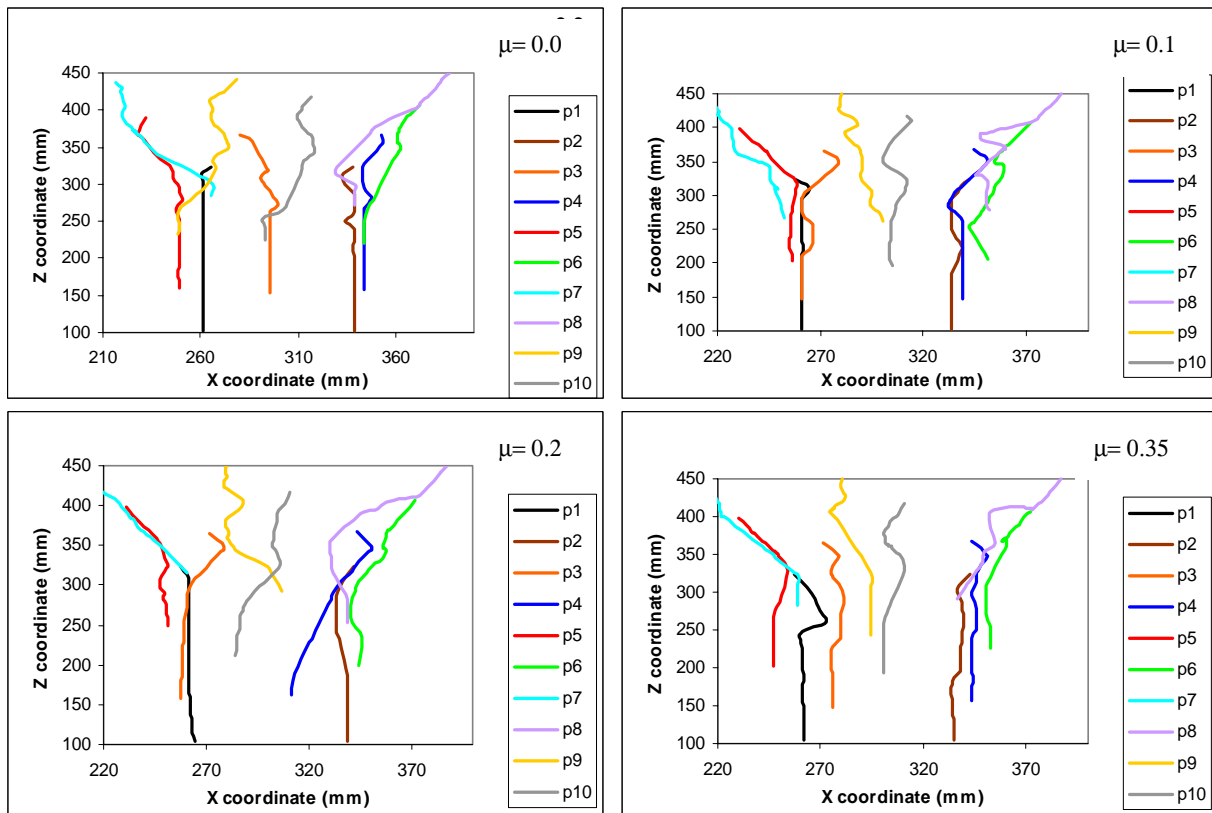
Fig. 4 Tracks of particle centroids from simulations using different coefficients of inter-particle friction.

11
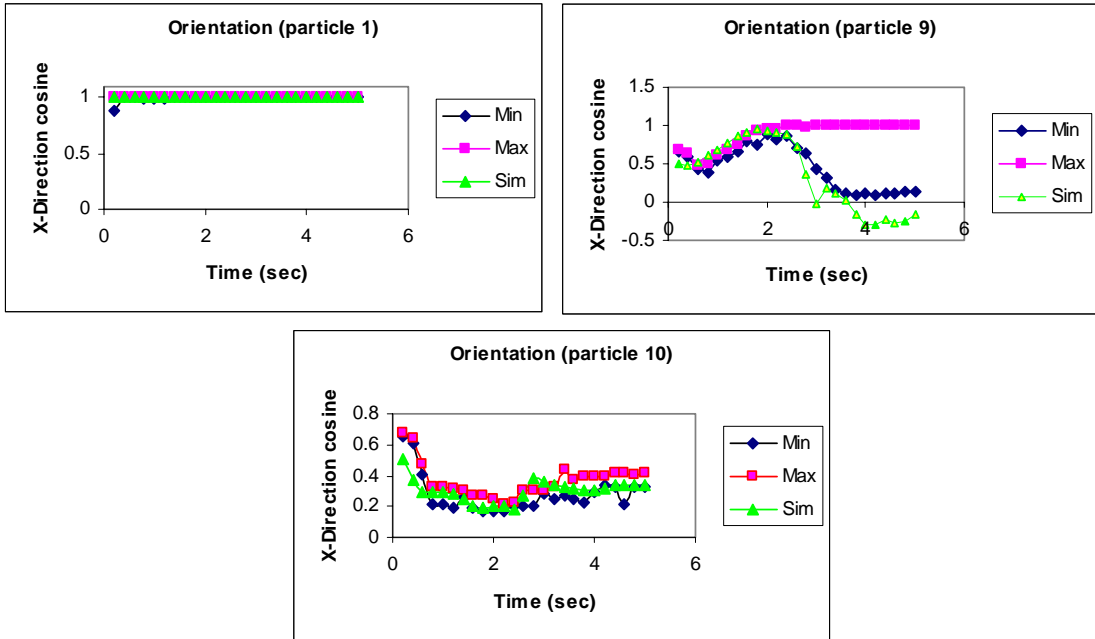
Fig 5   Change in particle orientation in experiment and simulation
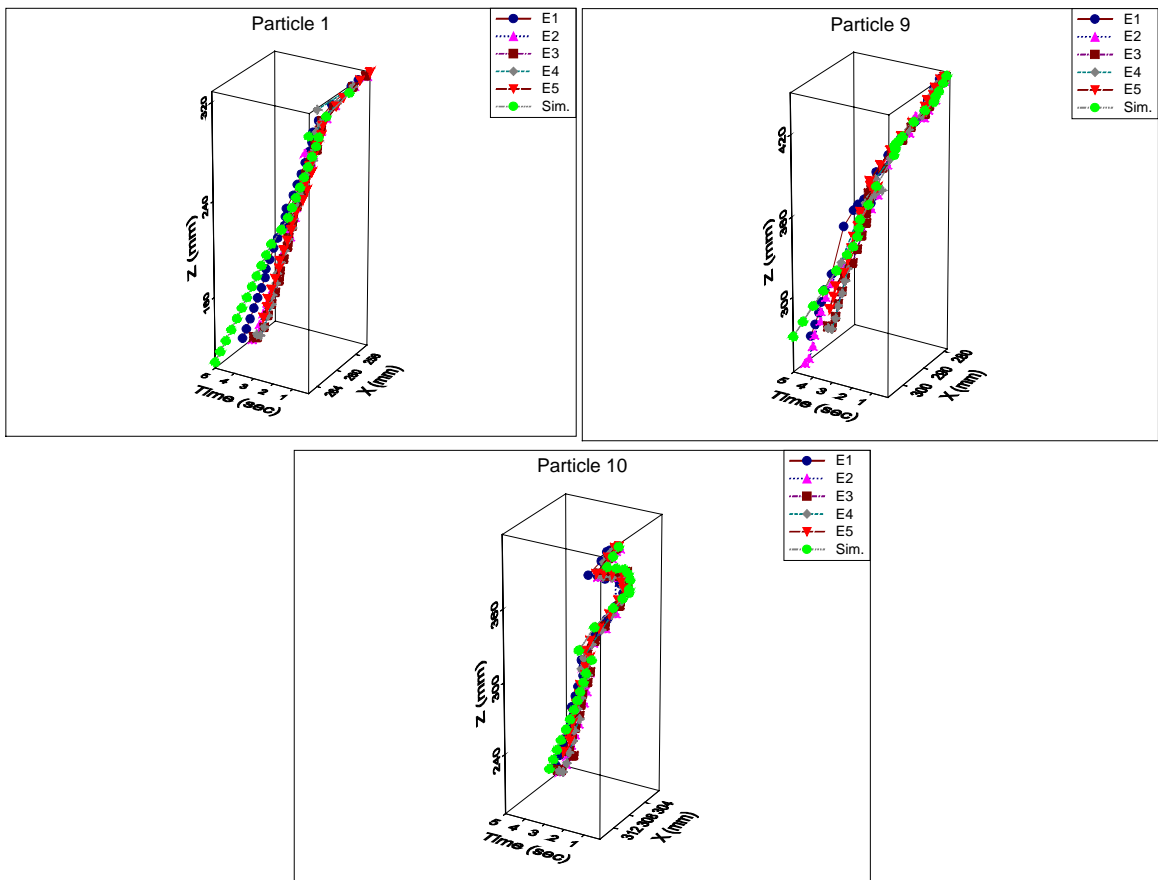
Fig 6 Particle trajectories in experiment and simulation
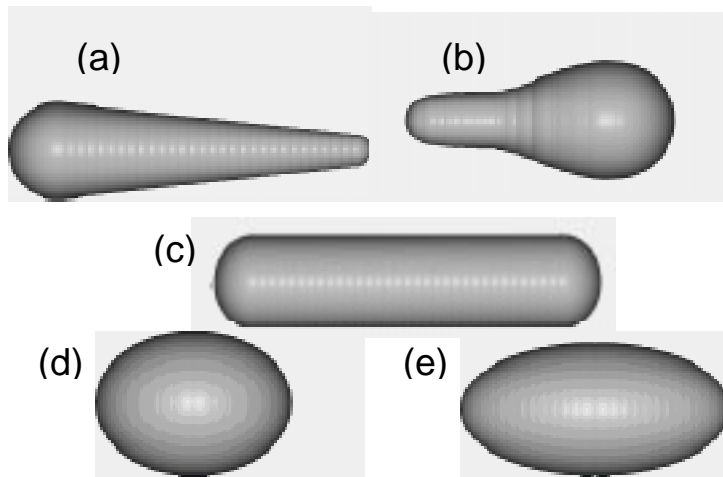
Fig 7   Examples of multi-element axi-symmetrical fruit shapes (a) tapered (30 element spheres), (b) irregular (12 element spheres), (c) cylindrical (20 element spheres), (e) 1.3:1 ellipsoid (18 element spheres) and (f) 2:1 ellipsoid (28 element spheres).
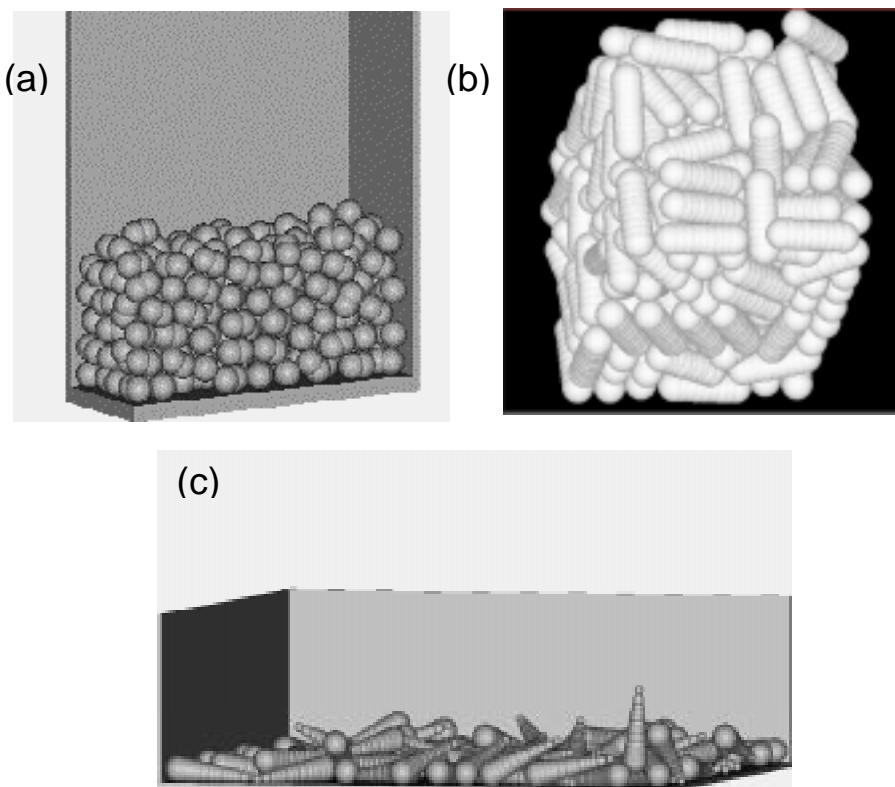
Fig 8   Examples of multi-element particle assemblies after random positioning and deposition under a gravity field; (a) 200 two-element particles, (b) 200 twenty-element cylindrical particles, and (c) 100 twelve-element tapered particles.